**The Report Committee for Sharon Xiangyi Chen**
**Certifies that this is the approved version of the following report**

# Design and Prototype of a Trimodal, Wireless, Neural Interface Device with Electrical and Electrochemical Neural Recording

**APPROVED BY**
**SUPERVISING COMMITTEE:**

Yaoyao Jia, Supervisor

Sensen Li

# Design and Prototype of a Trimodal, Wireless, Neural Interface Device with Electrical and Electrochemical Neural Recording

**by**

**Sharon Xiangyi Chen**

**Report**

Presented to the Faculty of the Graduate School of

The University of Texas at Austin

in Partial Fulfillment

of the Requirements

for the Degree of

**Master of Science in Engineering**

**The University of Texas at Austin**

**May 2023**

## Acknowledgements

I would like to thank my supervisor, Dr. Yaoyao Jia, for her guidance in being my supervisor as well as mentor during my time as a master's student. Her commitment to excellence inspires me to strive for higher standards in my work, I am grateful to have had this opportunity to work with her.

I also want to acknowledge my project collaborators: Isha Chakraborty, Ravi Akalkotkar, Daniel Krueger, Tristram Coffin, Mochen Hu, Xingjian Gan, and Swati Bhat. I would also like to thank Linran Zhao, who provided for us important advice and considerations during the design process.

# Abstract

## Design and Prototype of a Trimodal, Wireless, Neural Interface Device with Electrical and Electrochemical Neural Recording

Sharon Xiangyi Chen, MSE

The University of Texas at Austin, 2023

Supervisor: Yaoyao Jia

This report describes the design and prototype process of a wireless neural interface device that enables electrical and electrochemical data monitoring and closed-loop optogenetic stimulation to neural tissue through a graphical user interface (GUI). This system is designed to monitor and stimulate dopamine concentration in brain tissue. The electrical sensing front-end amplifies signals from 1Hz to 200Hz with a mid-band gain of 60dB (1000V/V). The chemical sensing front-end features an FSCV waveform generator with a 400V/s scan rate and a voltage sweep range of -0.25V to 1.36V. The optogenetic stimulation unit is a wirelessly controlled LED configurable for frequencies between 1Hz to 10Hz and an on-pulse time between 1 ms and 10 ms. The data acquisition rate for electrical and electrochemical sensing is 1kHz with 12-bit resolution. The wireless GUI connects to the neural interface device with a bidirectional wireless BLE link.

# Table of Contents

# List of Tables

# List of Figures

# Chapter 1: Introduction

Neurons in brain tissue communicate through both electrical and chemical signals. Electrical signals in neural tissue excite neurons to emit chemical signals called neurotransmitters to communicate with other neurons. [8] Some important neurotransmitters include dopamine, serotonin, and histamine, all of which are essential to human physical function and mental health. Currently, most neural interface devices only support electrical sensing for neural tissue. Though electrical signals can be an indicator of neurotransmitter activity, they do not give a targeted measurement of the chemical concentration of neurotransmitters in brain tissue. For mental health conditions characterized by a chemical imbalance in the brain, it is important to have accurate measurements of neural chemical concentration in real-time for targeted chemical balancing treatments. The treatment method we focus on in this paper is optogenetic stimulation, which uses targeted light stimulation to produce a response in mammalian brain tissue [10]. Some advantages of light stimulation over electrical stimulation for neural tissue include “cell-type specificity, sub-millisecond temporal precision, and rapid reversibility” of stimulus effects [6].

This report presents a neural interface circuit that features electrical and electrochemical sensing capabilities and closed-loop optogenetic stimulation. The target application of this circuit is to detect, monitor, and stimulate dopamine levels in mammalian brain tissue. The electrical and chemical sensor interface integrates into a larger system featuring a wireless graphical user interface (GUI) and an optogenetic stimulation unit. With the GUI, users can monitor sensor data and administer optogenetic stimulation in real time. The integrated sensing components, microcontroller, and

onboard wireless module consolidate into a small headstage circuit that fits on a rat's head.

This paper is structured as follows: Chapter 2 of this paper discusses some previous work on neural interface devices and introduces electrochemical sensing. Chapter 3 is a system overview to go into more detail about system design, simulation, and specifications. Chapter 4 presents measurement results, and Chapter 5 concludes the report and discusses future work based on this design.

# Chapter 2: Electrochemical Sensing Background

## PREVIOUS WORK

This project takes primary inspiration from two previous neural interface designs. The first device is an inductively-powered neural interface System on a Chip (SoC) that supports electrical neural recording, electrical stimulation, and optoelectronic stimulation. [12] This system is implantable and was tested on anesthetized rats in-vivo, which is a future goal of our system design. A notable capability of Jia's SoC is inductive powering. Battery-powered biomedical devices can be cumbersome for freely locomoting animal subjects, but Jia's work is powered by a wireless high-frequency inductive link that replaces battery power [12]. This functionality is of interest for future work on our design, as our design prototypes a wireless electrical and electrochemical recording device that is intended to be tested on freely locomoting rats.

The second device we took inspiration from is a wireless locomotive sensor that records neural and muscle electrical activity for closed-loop optogenetic stimulation. [6] This neural-locomotive sensor improves upon basic neural sensing functionality by adding wireless data transmission through a Bluetooth low energy (BLE) connection that

links to an external graphical user interface (GUI). The GUI is displayed on an electronic device and provides means for closed-loop optogenetic stimulation control. [6]

This current work takes inspiration from the functionalities of Jia and Zhao's designs including electrical neural recording, wireless BLE data transmission, and GUI-controlled optogenetic stimulation. Our system improves upon the previous designs by adding electrochemical recording capabilities.

### ELECTROCHEMICAL SENSING OVERVIEW

Electrochemical sensing is the characterization of chemical concentration through voltage and current measurements. One type of electrochemical sensing is Voltammetry, which is a method of applying a controlled voltage stimulus to an electrode and measuring the response current. When biological tissue is stimulated with an electrical charge, chemical reactions can occur and tissue impedance will change. Measuring the electrical response with respect to the fluctuating tissue impedance gives information about the chemical concentrations in the tissue. [1] Different chemicals react to different levels of voltage excitation, which allows us to selectively isolate and monitor the chemical(s) of interest. For example, monoamine neurotransmitters such as dopamine have a comparatively low oxidation voltage [4]. Therefore, applying a controlled low-voltage signal to brain tissue will produce a dopamine redox reaction and leave chemicals with higher redox potentials undisturbed. The isolated dopamine redox response allows us to find the dopamine concentration in neural tissue by measuring electrical current despite there being other chemicals present. [1]

Cyclic voltammetry (CV) is a type of voltammetry that works by applying a triangle-shaped stimulation voltage to a substance and reading the electrical current from the resulting redox reaction [2]. Traditional CV scan rates are on the order of 100mV/s,

which is too slow to characterize dopamine reactions. [2] The most common electrochemical sensing method for dopamine is Fast Scan Cyclic Voltammetry (FSCV), which features a pulsed triangle voltage at a scan rate of between 300V/S to 1000V/s [10]. FSCV is preferred over CV because FSCV scans complete within milliseconds and is fast enough to capture dopamine redox reaction characteristics [2]. Typically, FSCV implementations have a scan rate of 400V/s. The dopamine oxidation potential is around 0.6V and the reduction potential is around -0.1V. To stimulate dopamine oxidation and reduction responses, the FSCV voltage range applied to the tissue must include -0.1V and 0.6V [10]. Our electrochemical sensing system includes an FSCV waveform generator and a current sensing unit.

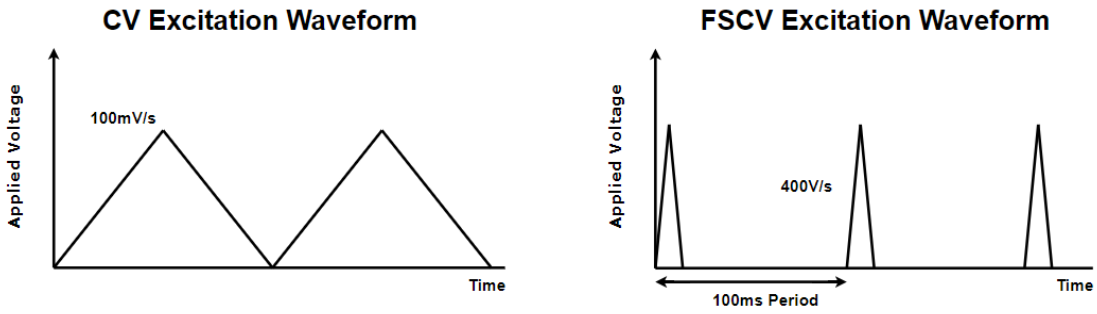


Figure 1: CV and FSCV Excitation Waveforms

The FSCV current response should resemble the following curves shown in Figure 2. FSCV scans produce non-negligible background current in proportion to the scan rate. [E] To isolate the dopamine current response for analysis, the background current must be subtracted from the current reading. Figure 2.1 shows the full current response with the background current. Figure 2.2 shows the isolated dopamine redox current after

subtracting the background current. Users can then find dopamine concentration from the isolated dopamine redox current curve.

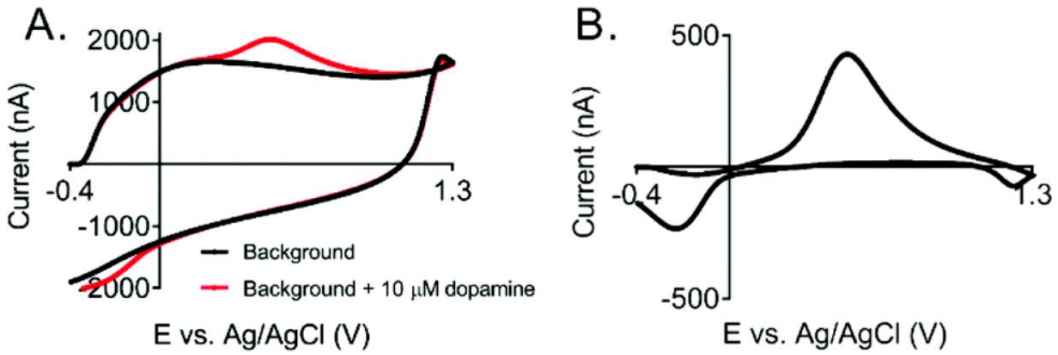


Figure 2: FSCV full current response (1), FSCV isolated dopamine redox current (2) [E]

**POTENTIOSTAT OVERVIEW**

The potentiostat is a common circuit used for Voltammetry measurements. It uses three electrode probes to stimulate chemical reactions and measure the current response of a substance. A functional diagram of a potentiostat is shown in Figure 3. A potentiostat works by driving an excitation voltage into a substance to stimulate a redox reaction, then measuring the electrical current in the substance. During the redox reaction, substance impedance will change based on the concentration of the chemical undergoing reduction and oxidation. The changing impedance will produce a current response, which in turn gives insight into the concentration of the redox chemical.

During circuit operation, the FSCV excitation current is sent through the control electrode (CE) to brain tissue to create an FSCV excitation voltage between the working electrode (WE) and reference electrode (RE). [1] The control amplifier (CA) and buffer network achieve this by forcing the voltage between RE and CE to be the same excitation voltage while the WE voltage is held at AC ground. The WE collects the current between

the electrodes and feeds it through a transimpedance amplifier (TIA) which outputs a voltage proportional to the redox current response. The equation for the TIA output voltage is shown below in equation 1.

$$\text{TIA:} \quad V_o = -R_f * \mathrm{I}_{in} \tag{1}$$

The TIA output voltage is then analyzed to find the chemical concentration. In our case, the TIA output voltage is fed to a microcontroller ADC for data processing.

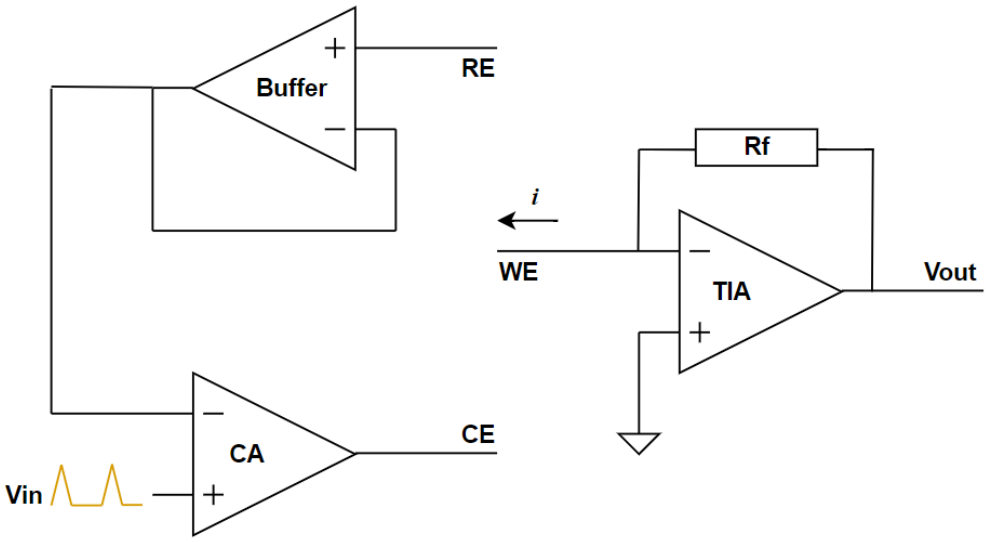


Figure 3: Basic Potentiostat Diagram

# Chapter 3: System Overview

Our neural interface system integrates an analog sensing front end and optoelectronic stimulation unit with a wireless software GUI for closed-loop neural sensing and stimulation. Figure 4 shows the full system block diagram with the suggested experimental setup.

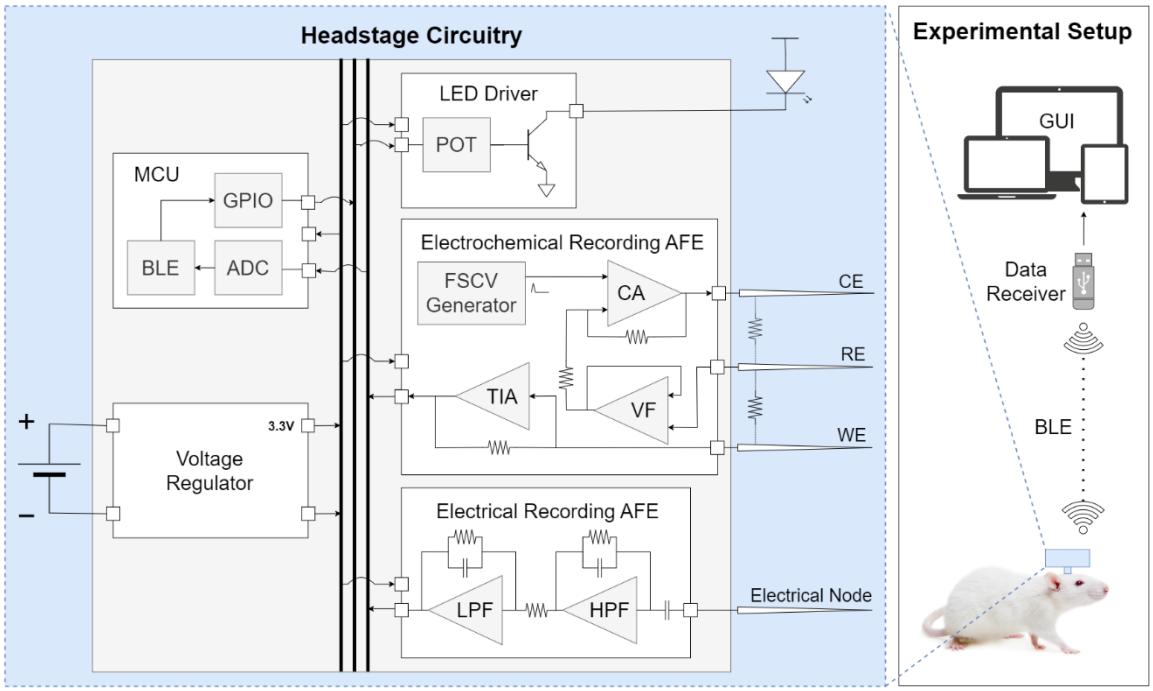


Figure 4: Full System Block Diagram

As shown above in Figure 4, the neural interface system is condensed into a small headstage that fits on the head of a rat. The four analog front-end (AFE) electrodes are designed to probe into the rat's brain tissue. The Electrical Recording AFE records electrical neural signals and the Electrochemical Recording AFE records the current response of dopamine redox reactions, which gives insight into dopamine concentration levels in the brain. The microcontroller unit (MCU) receives the recorded data from the

AFEs, converts it through an analog-to-digital converter (ADC), and wirelessly sends the recorded data to the graphical user interface (GUI) through a bidirectional Bluetooth Low Energy (BLE) link. The GUI plots the electrical and chemical data in real time and allows users to configure and administer optoelectronic stimulation to the brain tissue. If the user chooses to administer optoelectronic stimulation, the GUI sends the command through the BLE link to the MCU on the headstage, then the MCU adjusts the digital potentiometer (POT) in the LED driver to administer light stimulation to the rat's brain according to the user configuration. We will go into more detail about each headstage module in the following sections of this report.

## ELECTROCHEMICAL SENSING FRONT END

The chemical sensing front end for our dopamine detection unit consists of a potentiostat and a buffered FSCV voltage generator.

### FSCV Waveform Generator

The FSCV waveform generator is an op-amp integrator that receives two independent PWM signals at the input to create the pulsed FSCV triangle waveform. Figure 5 shows the circuit model for the FSCV triangle wave generator.

$$Vout = -\frac{1}{R_{in}C_f}\int_0^t Vin * dt \qquad 3$$

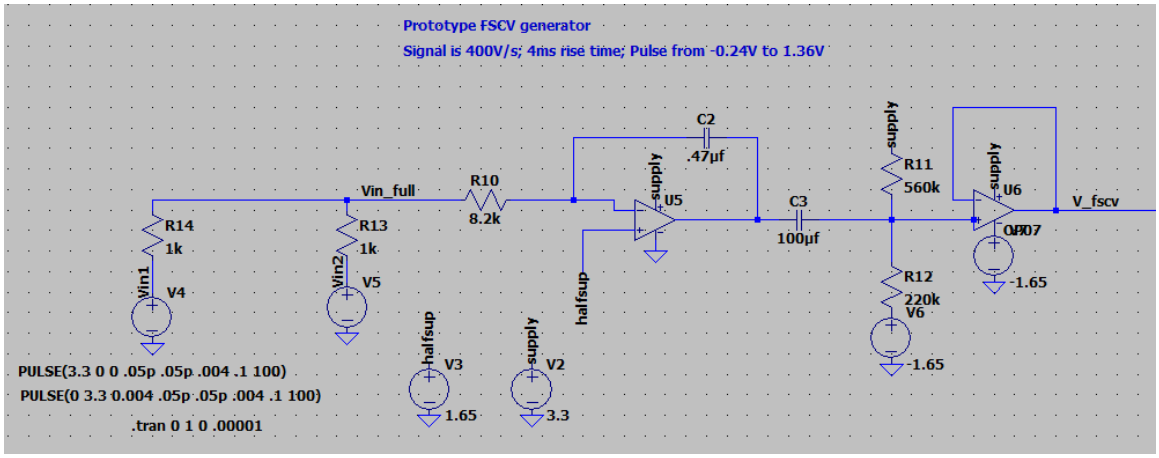


Figure 5: Op-Amp Integrator FSCV Waveform Generator Circuit Model

The Vout vs Vin relationship of an op-amp integrator is shown in Equation 3. A triangle pulse wave can be created by concatenating two lines, one with a positive slope and the other with a negative slope. To get a linear slope at Vout, Vin must be a square wave. This can be achieved with a summation of two PWM signals at the input of the integrator (vin_full in Figure 5), the FSCV voltage inputs are shown in Figure 6.

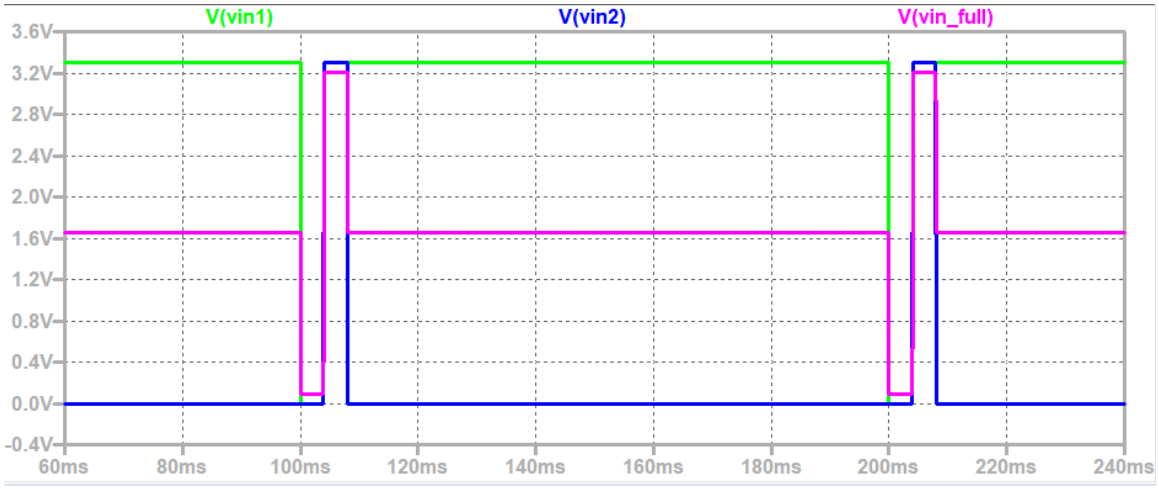


Figure 6: FSCV Waveform Generator Input PWMs and Integrator Input

Figure 7 shows the output FSCV waveform. The simulated triangle voltage pulse parameters are listed below in Table 1.

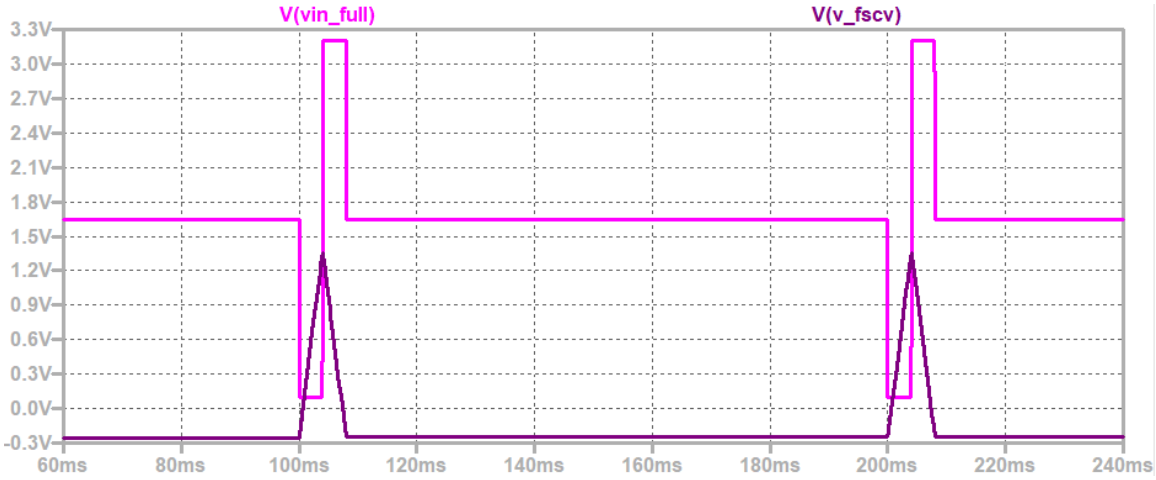


Figure 7: FSCV Waveform Generator Integrator Input and FSCV Output

| Parameter | Value |
|---|---|
| Voltage Range | [ -0.247V, 1.3628V ] |
| Rise/Fall Time | 4ms |
| Period | 100ms |
| Scan Rate | 402.45V/s |

Table 1: Simulated FSCV Parameters

**Potentiostat**

Our potentiostat LTSpice circuit model is shown in Figure 8. As described in the Electrochemical Sensing Background section, the expected electrode response during potentiostat operation is for the RE and CE voltage to be the same and the voltage difference between RE and WE to be the FSCV excitation signal. Figure 9 shows this response for the potentiostat model in Figure 8.

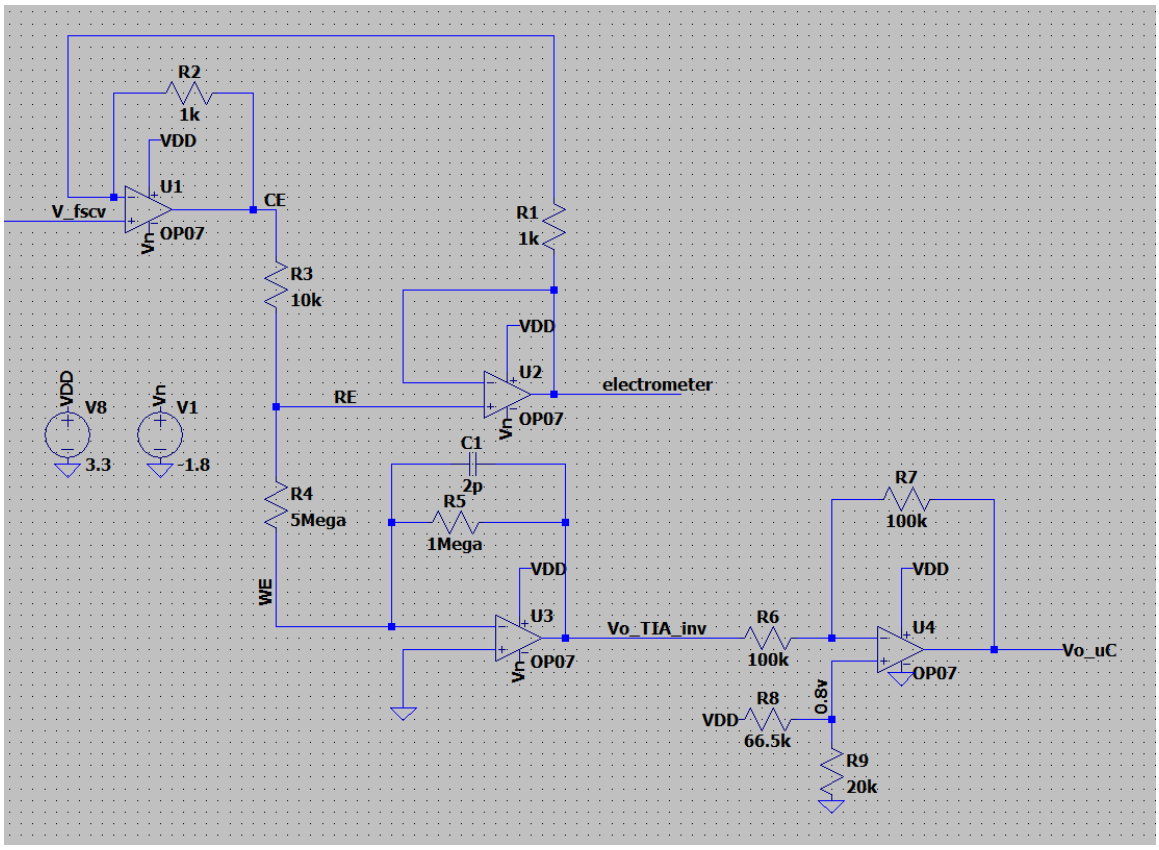


Figure 8: Potentiostat Circuit Model

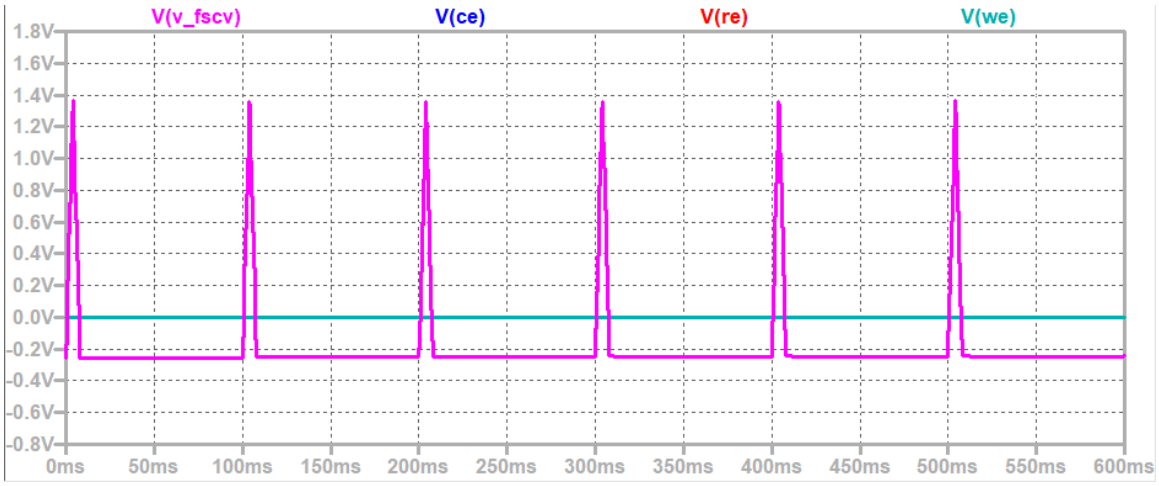


Figure 9: Plot of TIA voltage output V(vo_tia_inv)

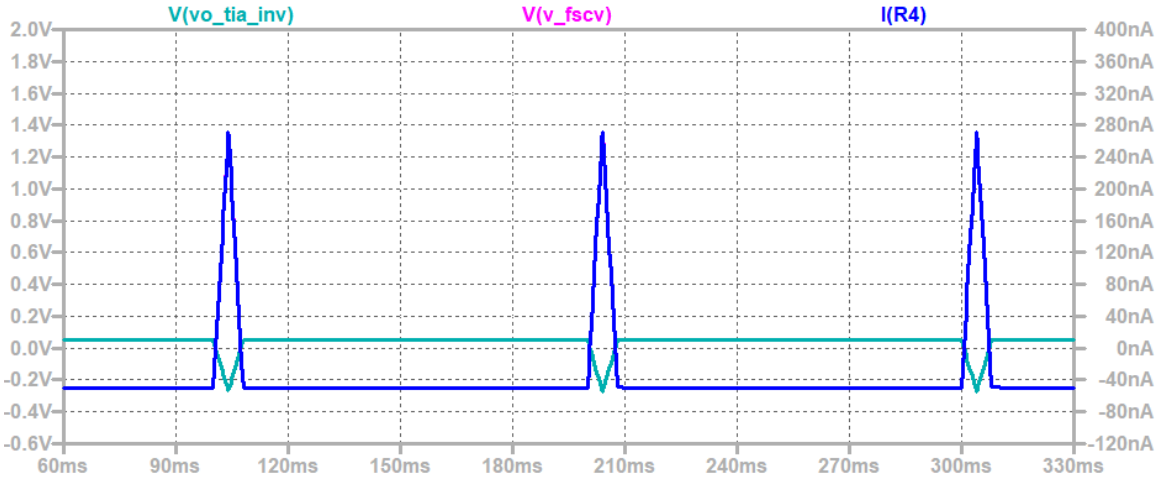


Figure 10: Plot of TIA voltage output V(vo_tia_inv), FSCV voltage input V(v_fscv), and WE current I(R4)

Figure 10 shows the FSCV input waveform compared to the transimpedance measurement (see equation 2). Note that $R_f$ is R5 on the circuit model in Figure 8, which gives us a transimpedance gain of 120dB (1MOhms).

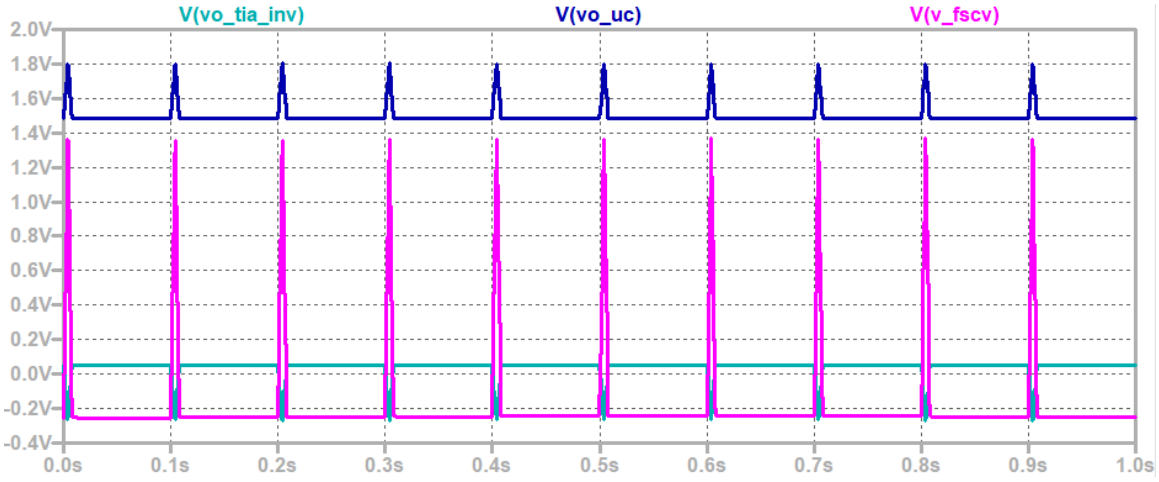


Figure 11: Plot of FSCV input (v_fscv), TIA output V(vo_tia_inv), and Microcontroller Input Voltage V(vo_uc)

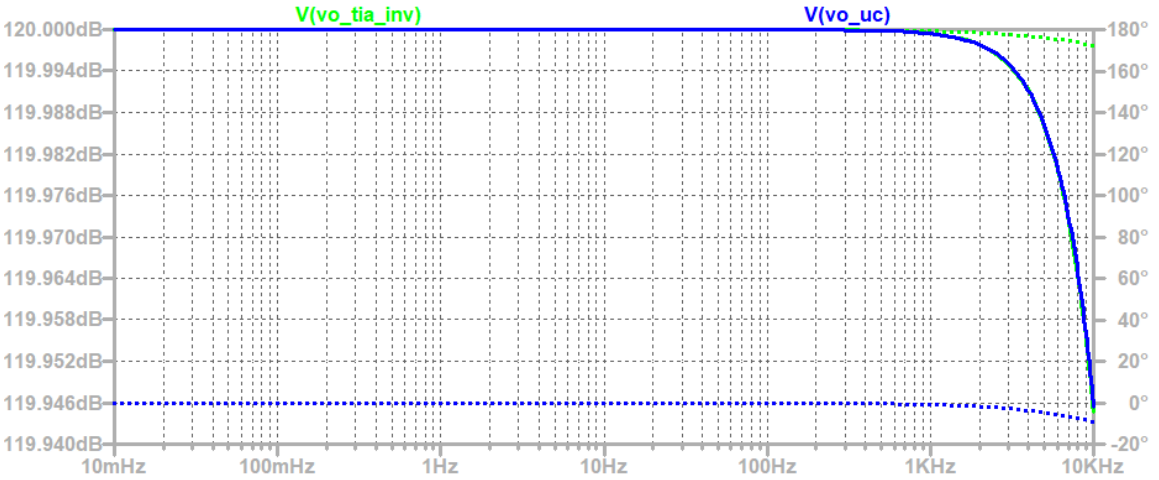


Figure 12: Frequency Response of TIA output V(vo_tia_inv) and Microcontroller Input Voltage V(vo_uc)

The unity gain inverting amplifier at the TIA output corrects the inverted output voltage from the TIA as shown in Figure 11. This ensures that the microcontroller ADC receives a positive voltage with respect to positive current from the electrochemical cell.

The frequency response of the TIA is shown in Figure 12, as expected, the gain is 120dB within 1kHz. The feedback capacitor in the TIA filters high-frequency noise and adds the 1kHz break frequency to the TIA frequency response.

This potentiostat design functions as expected according to simulation results with fixed impedance between the electrodes. This potentiostat model built in simulation does not show the expected FSCV current response in Figure 2 because the impedance between RE and WE is fixed in the simulation. During an FSCV scan, the tissue impedance will change because of the stimulated redox reaction, which in turn will change the current level and produce the expected FSCV current waveform.

**ELECTRICAL SENSING FRONT END**

Neuron activity typically has frequencies between 0.1Hz to 80Hz and voltages within 10mV [9]. A bandpass filter with a midband gain of around 1000V/V (60dB) can be used to capture neural electrical activity. The electrical front-end circuit diagram is shown below in Figure D. This topology features a Band-Pass filter (BPF) built with a High-Pass filter (HPF) in series with a Low-Pass filter (LPF). The frequency response equations for the electrical sensor front end and break frequencies are shown in equations (1), (2), and (3).

Our specifications are as follows: Ho = 1000V/V = 60dB; $f_{HPF}$ = 1Hz; $f_{LPF}$ = 200Hz. The circuit component values are constrained by the filter specifications and frequency response equations. The chosen components are shown in Figure 13.

$$\text{HPF Transfer Function: } HPF\text{: } H_{HP}(s) = -\frac{sR_fC_{in}}{(1+sR_fC_f)} \quad \omega_H = \frac{1}{R_fC_f} \qquad (1)$$

$$\text{LPF Transfer Function: } H_{LP}(s) = -\frac{R_f}{R_{in}}\frac{1}{(1+sR_fC)} \qquad \omega_L = \frac{1}{R_fC} \tag{2}$$

$$\text{Full BPF Response: } H_{HP}(s) * H_{LP}(s) = \frac{R_{fLP}}{R_{inLP}}\frac{sR_{fHP}C_{inHP}}{\left(1+sR_{fHP}C_{fHP}\right)(1+sR_{fLP}C_{LP})} \tag{3}$$

$$f_{HPF} = \frac{1}{2\pi * R_{fHP}C_{fHP}} \qquad f_{LPF} = \frac{1}{2\pi * R_{fLP}C_{LP}}$$

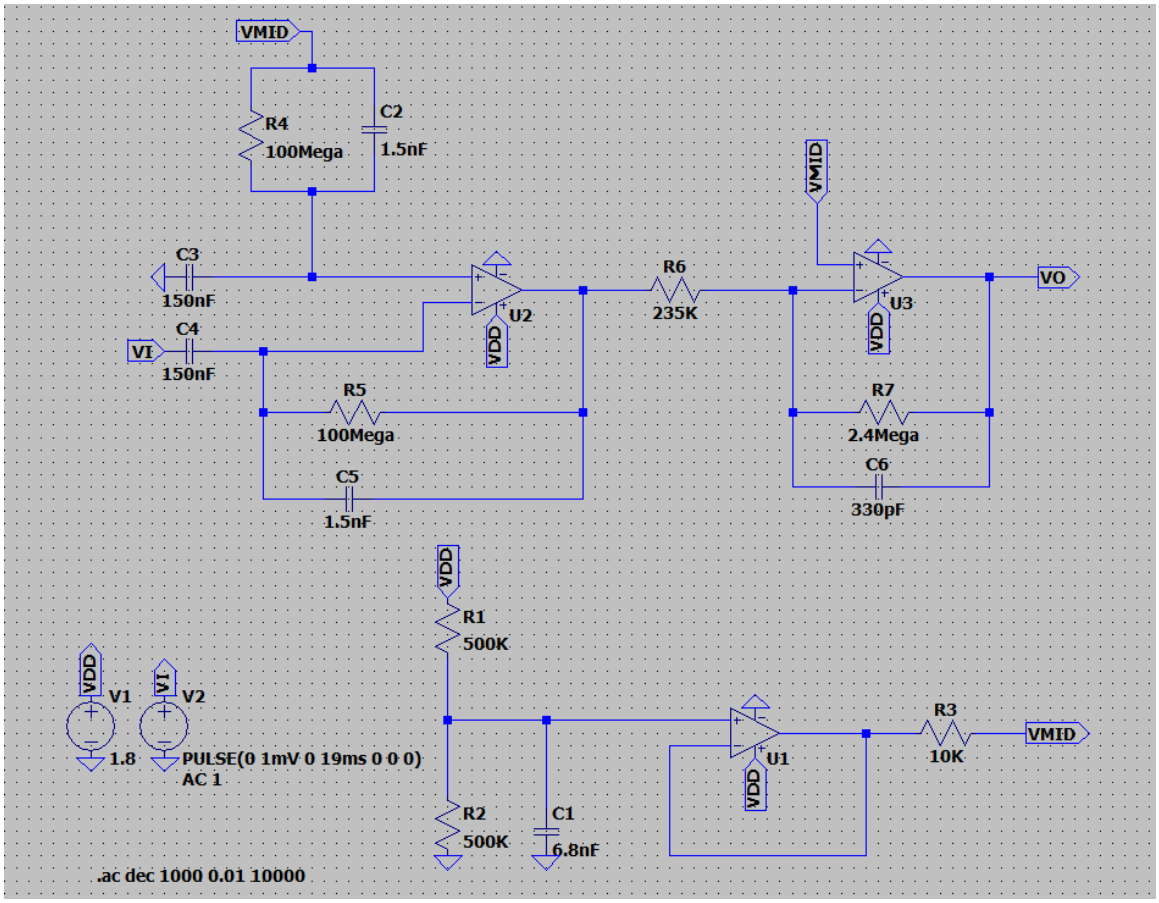


Figure 13: Electrical Sensing Front End Circuit Model

The circuit model shown in Figure 13 has an active high pass filter at the first stage (U2) and an active low pass filter at the second stage (U3). Note that Vo from the electrical sensing front end is processed by a microcontroller that reads only positive voltages, so the sensor output voltage is offset by half of VDD to ensure that Vo stays in the positive voltage range. This is achieved with a buffered voltage divider (U1) that outputs a DC offset voltage of VDD/2 for the LFP and HPF.

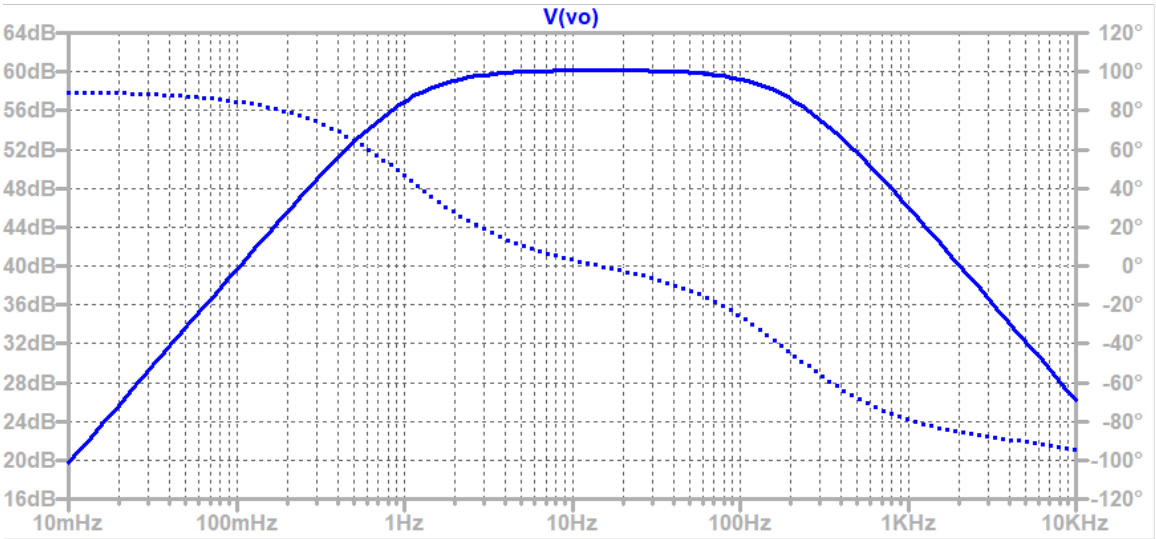


Figure 14: Electrical Sensing Front-End Frequency Response

**MCU FIRMWARE**

The microcontroller firmware dataflow chart is shown in Figure 15. When the system is in operation, the Headstage MCU collects data and administers LED stimulation while the USB MCU handles wireless data reception and interfaces with the GUI on an external electronic device. The two MCUs communicate through a bidirectional BLE link.

The Headstage MCU polls for data from the electrical and chemical front end at a rate of 1kHz with 12-bit data resolution. The collected data is consolidated in 25-bit data packets that include electrical data, electrochemical data, and LED on or off status. 7 additional bits are added to each data packet to track data loss. Each data packet sent to the USB MCU is 32 bits (4Bytes).

The USB MCU is plugged into an electronic device. When it receives the 4 Byte data packet, it parses and sends the data to the GUI through the UART protocol. If the user chooses to administer LED stimulation from the GUI, the GUI sends UART data to the USB MCU, which then sends a wireless BLE command to the Headstage MCU to engage the LED stimulus. The Headstage MCU controls the LED brightness and duty cycle using PWM signals and a serial peripheral interface (SPI) connection to a digital potentiometer. For more details on the LED stimulation unit, see the LED Stimulation Unit section in this report.

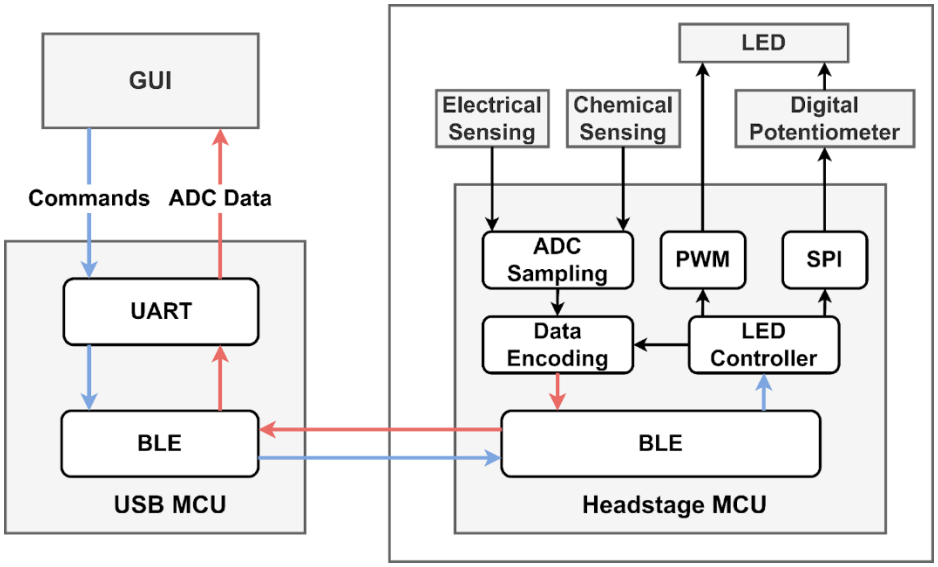


Figure 15: MCU Firmware Dataflow Diagram [5]

## GRAPHICAL USER INTERFACE

The GUI features two main components, the first being the plotting area for the recorded electrical data, chemical data, and LED on/off status, and the second is the user control panel with buttons for data acquisition, data plotting, and enabling LED stimulation. Figure 16 shows a screenshot of the interactive GUI.

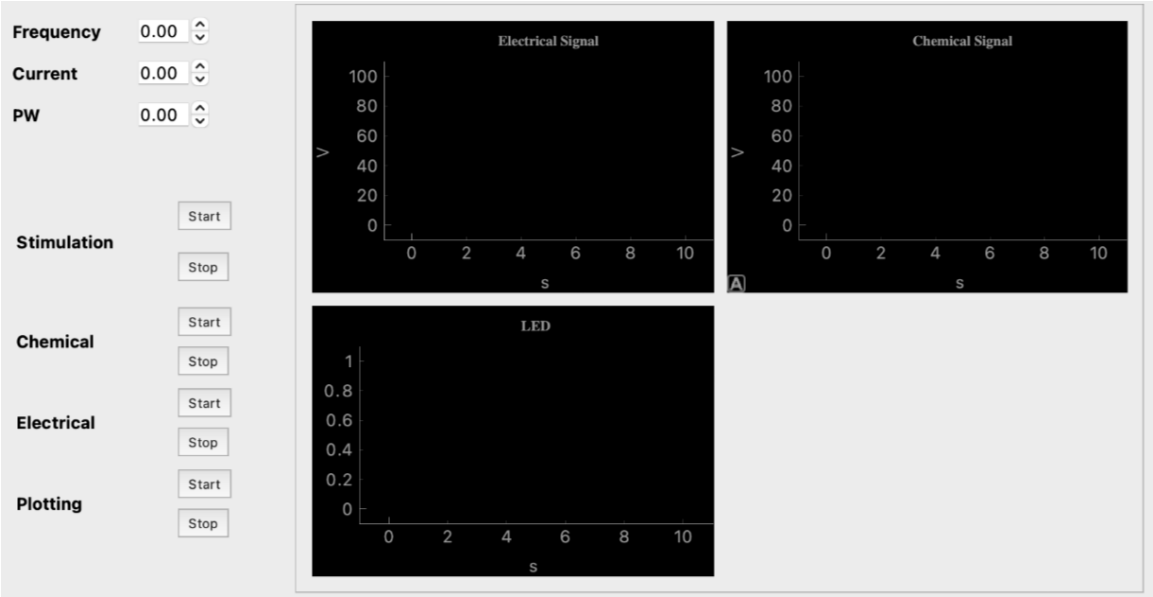


Figure 16: Graphical User Interface for Data Plotting and Optoelectronic Stimulation

As shown in Figure G, the left side control panel has an LED configuration section on the top to control the LED brightness and duty cycle. The start and stop buttons next to ‘Stimulation’ turn the LED on and off. The remaining three sets of buttons for chemical, electrical, and plotting control data updates for their respective graphs in the plotting area. All graphs are plotted with respect to time. The Electrical and Chemical plots are measured in voltage, and the LED plot shows the on/off status over time.

As described in the MCU firmware section, the Headstage MCU wirelessly sends data packets to the USB MCU through a BLE link, and the GUI receives the data from the USB MCU through a UART connection. The GUI then parses the data and places it in a data buffer. When the user presses ‘start’ to update the GUI plots, the most recent and complete data in the buffer will be displayed. The GUI’s data processing backend is programmed in Python, and the user interface display is programmed with PyQt.

### LED STIMULATION UNIT

The LED stimulation unit administers optoelectronic stimulation and consists of an LED bulb, a digital potentiometer, and a BJT transistor. The digital potentiometer connects in series with the base of the BJT to adjust the brightness of the LED by controlling BJT base current. Both LED current and LED pulse width are configurable through the GUI. When the Headstage MCU receives the LED configurations, it sets the digital potentiometer resistance with an SPI connection to control the LED current. To adjust LED pulses, users can set LED pulse frequency between 1-10Hz and pulse widths between 1-10ms from the GUI. See Figure 4 for the block diagram of the LED stimulation unit connected with the full system.

# Chapter 4: Prototyping and Measurement Results

We created an evaluation module (EVM) to test the system design. The EVM features a 5cm x 10cm motherboard that has pin connections for the four peripheral modules: Electrical sensing AFE, Chemical sensing AFE, LED Driver, and FSCV waveform generator (Refer to Figure 4: Full System Block Diagram). Figure 17 shows the four peripheral modules connected to the EVM motherboard.

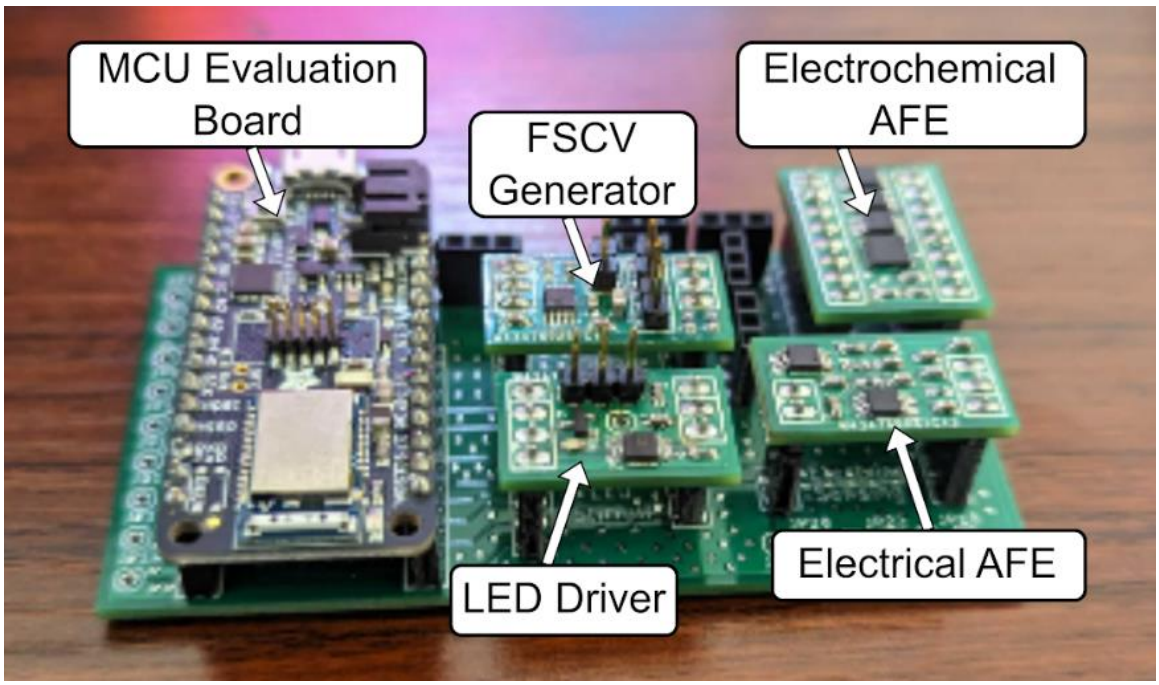


Figure 17: MCU Connector EVM Motherboard PCB with Peripheral Boards

To test sensing functionality, we measured the previously defined specifications of electrical sensing front end and electrochemical sensing front end.

As described above in the Electrical Sensing Front End section, the most critical performance measures for electrical neural sensing are the midband gain and bandwidth. Recall that the expected gain and bandwidth should be 1000V/V (60dB) and between

1Hz and 200Hz. To test the gain and bandwidth, we emulated neural voltage signal amplitude and frequency with a waveform generator and measured the midband gain to be 61.7dB and -3dB frequencies of 1.587Hz and 77Hz. Figure 18 shows the measured frequency response of the Electrical Sensing Front-End.

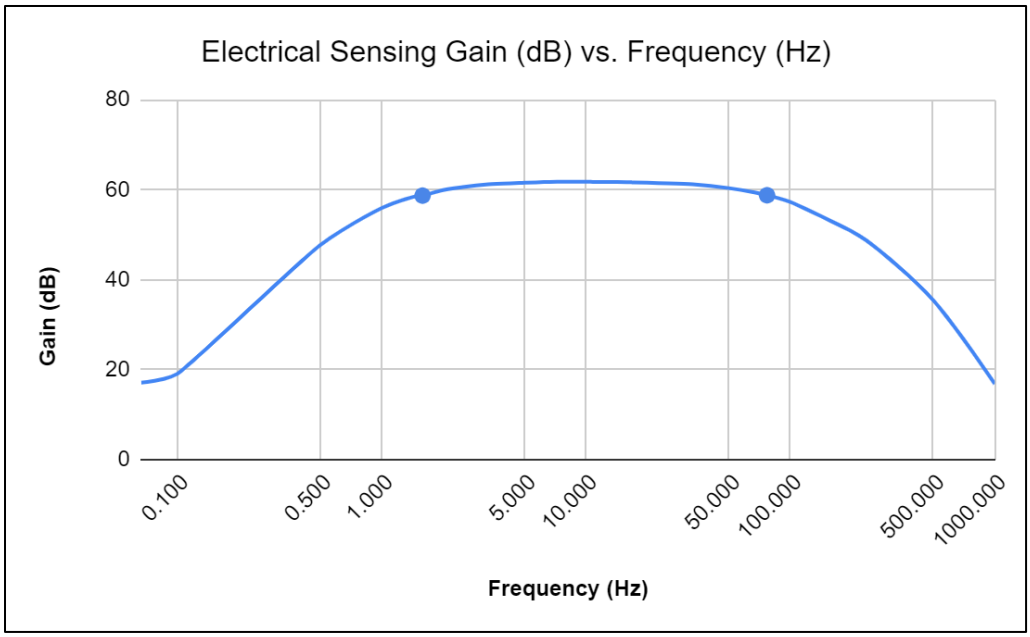


Figure 18: Measured Electrical Sensing Front-End Frequency Response

The Chemical Sensing Front End has two components, the FSCV waveform generator and the potentiostat. We first measured the FSCV waveform generator output. The triangle wave output ranged from 0.25V to 1.36V and had a rise/fall time of 4.1ms, which gives a scan rate of 392.7V/s. To ensure potentiostat functionality, we checked that the output voltage of the TIA is a low amplitude inverted FSCV signal that matches the simulation TIA output waveform. The TIA output is then fed through an inverting amplifier to produce a noninverted signal with adjustable gain. The inverting amplifier output is processed by the microcontroller ADC and sent to the GUI for display. The

measured TIA gain is 1,000,000V/V (120dB). The large gain is to account for dopamine redox currents that are on the magnitude of 0.1uA. Any gain adjustments after the TIA can be achieved by changing the resistor ratio of the inverting amplifier (Refer to the Potentiostat Circuit Model in Figure E, U4 is the inverting amplifier at the output of the TIA). Figure 18 shows the measured TIA output and microcontroller input from the electrochemical sensing module:

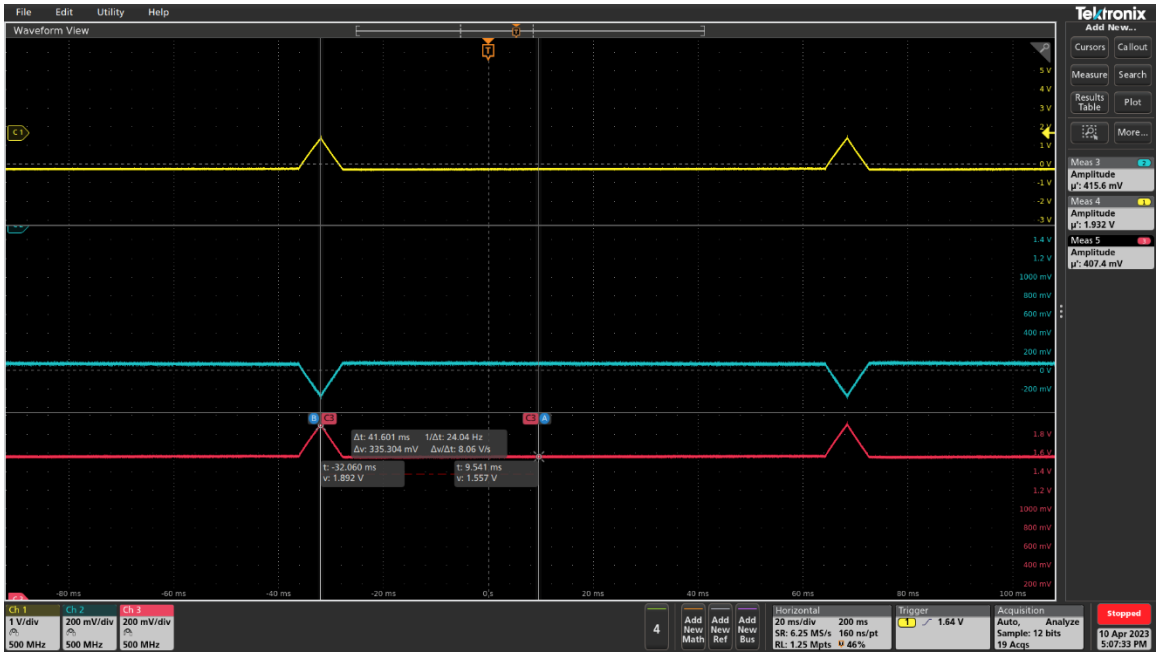


Figure 19: Electrochemical Sensing EVM measurements: Yellow = FSCV input, Blue = TIA output, Red = uController Input

The rest of the specifications are system-level parameters set in firmware. Our measured system specifications from the EVM are listed in Table 2.

| Subsystem | Parameter | Specification | Simulation | Measurement |
|---|---|---|---|---|
| Electrical Sensing Front End | Midband Gain | 60dB | 60dB | 61.7 dB |
| | Low Cutoff Frequency | 1Hz | 1Hz | 1.587 Hz |
| | High Cutoff Frequency | 200Hz | 200Hz | 77 Hz |
| Electrochemical Sensing Front End | PWM1 Pulse Width | 4ms | 4ms | 4.25ms |
| | PWM2 Pulse Width | 4ms | 4ms | 7.25ms |
| | FSCV Slope | 400V/s | 402.45V/s | 392.7V/s |
| | FSCV Period | 100ms | 100ms | 100 ms |
| | FSCV Voltage Range | [-0.4V, 1V] | [ -0.25V, 1.36V ] | [-0.25V, 1.36V] |
| | FSCV Rise Time | 4ms | 4ms | 4.1ms |
| | Transimpedance Gain | 120dB | 120dB | 122.2dB |
| Optical Stimulation | On-Pulse Range | [1ms, 10ms] | - | [1ms, 10ms] |
| | Frequency Range | [1Hz, 10Hz] | - | [1Hz, 10Hz] |
| Headstage MCU | ADC Sampling Rate | 1kHz | - | 1kHz |
| | Data Resolution | 12 bit | - | 12 bit |
| BLE Link | Data Throughput | 32 kbps | - | 32 kbps |

Table 2: Practical System Specification Parameters

# Chapter 5: Conclusion and Future Work

This report presented a prototype design of a neural interface device that monitors and stimulates dopamine levels in neural tissue in a closed-loop manner. Our device is capable of electrical recording, electrochemical recording, optogenetic stimulation, and wireless BLE pairing to an external GUI for user control. The sensor front ends offer suitable gain and bandwidth to accurately measure and record data on the order of nA and mV, which is the neural signal range. Users can administer optogenetic stimulation in real-time and monitor electrical and chemical data through the wireless GUI.

Our current design is a prototype version of an integrated implantable neural interface device. It establishes proof of concept for future neural interface systems that integrate closed-loop neural stimulation, electrical recording, electrochemical recording, and wireless monitoring for a fuller characterization of neural dopamine activity. In the future, we plan to test this design in-vitro on muscular tissue and in-vivo on a live rat. We also plan to integrate this system on a chip (SoC) to make an implantable, trimodal, wireless neural interface device.

# References


[1] A. Scozzari, “Electrochemical Sensing Methods: A Brief Review,” *SpringerLink*, 01-Jan-1970. [Online]. Available: https://link.springer.com/chapter/10.1007/978-1-4020-8480-5_16. [Accessed: 22-Mar-2023].

[2] B. J. Venton and Q. Cao, “Fundamentals of fast-scan cyclic voltammetry for dopamine detection,” *The Analyst*, vol. 145, no. 4, pp. 1158–1168, 2020.

[3] D. H. Kim, Y. Oh, H. Shin, C. D. Blaha, K. E. Bennet, K. H. Lee, I. Y. Kim, and D. P. Jang, “Investigation of the reduction process of dopamine using paired pulse voltammetry,” *Journal of Electroanalytical Chemistry*, vol. 717-718, pp. 157–164, 2014.

[4] “FAST scan cyclic voltammetry of dopamine and serotonin in mouse brain ...,” *Electrochemical Methods for Neuroscience.* [Online]. Available: https://www.ncbi.nlm.nih.gov/books/NBK2579/. [Accessed: 02-Apr-2023].

[5] I. Chakraborty, R. Akalkotkar, D. Krueger, T. Coffin, M. Hu, X. Chen, X. Gan, S. Bhat, L. Zhao, and Y. Jia, “A Wireless Trimodal Neural Interface Device with Electrical and Electrochemical Recording,” *2023 IEEE Texas Symposium on Wireless and Microwave Circuits and Systems (WMCS)*.

[6] L. Zhao, Y. Gong, W. Li, and Y. Jia, “Wireless Multimodal Neural Interface Device For Neural Control Studies,” *2021 IEEE Biomedical Circuits and Systems Conference (BioCAS)*, 2021.

[7] “Neurons,” *Organismal Biology*. [Online]. Available: https://organismalbio.biosci.gatech.edu/chemical-and-electrical-signals/neurons/#:~:text=Neurons%20communicate%20via%20both%20electrical,one%20neuron%20to%20the%20next. [Accessed: 02-Apr-2023].

[8] “Neurons,” *Organismal Biology*. [Online]. Available: https://organismalbio.biosci.gatech.edu/chemical-and-electrical-signals/neurons/. [Accessed: 25-Mar-2023].

[9] R. Martinek, M. Ladrova, M. Sidikova, R. Jaros, K. Behbehani, R. Kahankova, and A. Kawala-Sterniuk, “Advanced bioelectrical signal processing methods: Past, present and future approach—part I: Cardiac signals,” *Sensors*, vol. 21, no. 15, p. 5186, 2021.

[10] . Chen, A. Canales, and P. Anikeeva, “Neural Recording and Modulation Technologies,” *Nature Reviews Materials*, vol. 2, no. 2, 2017.

[11] S. Z. M. R. V. P. LS; “Physiology, neurotransmitters,” *National Center for Biotechnology Information*. [Online]. Available: https://pubmed.ncbi.nlm.nih.gov/30969716/. [Accessed: 25-Mar-2023].

[12] Y. Jia, U. Guler, Y.-P. Lai, Y. Gong, A. Weber, W. Li, and M. Ghovanloo, “A trimodal wireless implantable neural interface system-on-chip,” *IEEE Transactions on Biomedical Circuits and Systems*, vol. 14, no. 6, pp. 1207–1217, 2020.